THE JOURNAL OF BIOLOGICAL CHEMISTRY VOL. 284, NO. 42, pp. 28660–28673, October 16, 2009
Printed in the U.S.A.

The Metastasis Efficiency Modifier Ribosomal RNA Processing 1 Homolog B (RRP1B) Is a Chromatin-associated Factor*[S]

Received for publication, May 20, 2009, and in revised form, July 29, 2009 Published, JBC Papers in Press, August 26, 2009, DOI 10.1074/jbc.M109.023457

Nigel P. S. Crawford[1], **Hailiu Yang, Katherine R. Mattaini, and Kent W. Hunter**[2]

From the Laboratory of Cancer Biology and Genetics, National Cancer Institute, National Institutes of Health, Bethesda, Maryland 20892

There is accumulating evidence for a role of germ line variation in breast cancer metastasis. We have recently identified a novel metastasis susceptibility gene, *Rrp1b* (ribosomal RNA processing 1 homolog B). Overexpression of *Rrp1b* in a mouse mammary tumor cell line induces a gene expression signature that predicts survival in breast cancer. Here we extend the analysis of RRP1B function by demonstrating that the *Rrp1b* activation gene expression signature accurately predicted the outcome in three of four publicly available breast carcinoma gene expression data sets. In addition, we provide insights into the mechanism of RRP1B. Tandem affinity purification demonstrated that RRP1B physically interacts with many nucleosome binding factors, including histone H1X, poly(ADP-ribose) polymerase 1, TRIM28 (tripartite motif-containing 28), and CSDA (cold shock domain protein A). Co-immunofluorescence and co-immunoprecipitation confirmed these interactions and also interactions with heterochromatin protein-1α and acetyl-histone H4 lysine 5. Finally, we investigated the effects of ectopic expression of an *RRP1B* allelic variant previously associated with improved survival in breast cancer. Gene expression analyses demonstrate that, compared with ectopic expression of wild type *RRP1B* in HeLa cells, the variant *RRP1B* differentially modulates various transcription factors controlled by TRIM28 and CSDA. These data suggest that *RRP1B*, a tumor progression and metastasis susceptibility candidate gene, is potentially a dynamic modulator of transcription and chromatin structure.

The concept of germ line polymorphism as a significant variable in susceptibility to metastasis in breast cancer is gaining wider acceptance in the scientific community (1). Given that breast carcinoma is the most common form of cancer in women in the United States (2) and that the majority of breast cancer-related deaths are attributable to metastasis, the importance of exposing factors influencing this process is clear. Our initial studies have focused upon utilization of the highly metastatic polyoma middle T model of mouse mammary tumorigenesis (3) to define germ line elements modulating metastasis susceptibility (4). Combined experimental approaches, spearheaded by quantitative trait locus mapping, facilitated the identification of the first known metastasis susceptibility gene, *Sipa1* (signal-induced proliferation antigen 1) (5, 6). *Sipa1* encodes a protein with Rap1 GTPase-activating protein activity and contains a polymorphism in a PDZ protein-protein interaction domain that renders different strains of laboratory mice differentially susceptible to metastasis (5).

Subsequent studies were based on two observations: that 1) knockdown of *Sipa1* dysregulates the expression of extracellular matrix (ECM)[3] genes,[4] and 2) ECM genes are frequent components of prognostic microarray gene expression profiles observed in both human breast cancer (*e.g.* Refs. 7–9) and mouse models of mammary tumorigenesis (10–12). Expression QTL mapping in the AKXD panel of recombinant inbred mice (13) was performed to determine whether the loci driving metastasis susceptibility and differential ECM gene expression in tumors more prone to metastasizing were one and the same (14). Seven genes were found to have a significant role in the modulation of metastasis predictive ECM gene expression in AKXD mice (15). However, two genes appeared to have particularly profound effects upon global transcription patterns: the bromodomain factor *Brd4* and a gene of unknown function, *Rrp1b*. Significantly, both of these factors physically interact with SIPA1, with BRD4 binding increasing (16) and RRP1B binding decreasing (14) the Rap1 GTPase-activating protein activity of SIPA1.

Subsequently, ectopic expression of either *Rrp1b* or *Brd4* was found to significantly suppress the metastatic capacity of the highly aggressive Mvt-1 mouse mammary tumor cell line and to induce gene expression signatures that can predict survival in breast cancer (14, 17). Examination of Mvt-1/*Rrp1b* microarray data reveals that ectopic expression of *Rrp1b* significantly impacts over 1,300 genes (14). Furthermore, quantitative real time PCR analysis of these and similar cell lines reveals that *Rrp1b* dysregulation alters the expression of numerous metastasis-related factors, most notably ECM genes (14). Given these

* This work was supported, in whole or in part, by the National Institutes of Health, NCI, Center for Cancer Research, Intramural Research Program.

[S] The on-line version of this article (available at http://www.jbc.org) contains supplemental Tables S1–S5 and Figs. S1 and S2.

[1] Present address: Cancer Genetics Branch, National Human Genome Research Institute, National Institutes of Health, Bethesda, MD 20892.

[2] To whom correspondence should be addressed: Laboratory of Cancer Biology and Genetics, CCR/NCI/NIH, Bldg. 37, Rm. 5046, 37 Convent Dr., Bethesda, MD 20892-4264. Tel.: 301-435-8957; Fax: 301-480-2772; E-mail: hunter@mail.nih.gov.

[3] The abbreviations used are: ECM, extracellular matrix; HA, hemagglutinin; TEV, tobacco etch virus; MS, mass spectrometry; HPLC, high pressure liquid chromatography; co-IP, co-immunoprecipitation; CEB, chromatin extraction buffer; qPCR, quantitative real time PCR; bis-tris, 2-[bis(2-hydroxyethyl)amino]-2-(hydroxymethyl)propane-1,3-diol; MOPS, 4-morpholinepropanesulfonic acid; MES, 4-morpholineethanesulfonic acid; PBS, phosphate-buffered saline; DAPI, 4′,6-diamidino-2-phenylindole; PIPES, 1,4-piperazinediethanesulfonic acid; TAP, tandem affinity purification; co-IF, co-immunofluorescence; P-TEFb, positive transcription elongation factor b; KRAB, Krüppel-associated box; ZNF, zinc finger.

[4] K. W. Hunter, unpublished observations.

profound changes in gene expression, we hypothesize that *Rrp1b* is a modulator of global gene expression.

In the current study, we demonstrate that the previously described Mvt-1/*Rrp1b* prognostic signature can be used to predict breast cancer-specific survival in multiple breast cancer expression data sets. A number of potential mechanisms by which *Rrp1b* modulates global gene expression are revealed through protein-protein interaction analyses, with tandem affinity purification being used to investigate the function of this very poorly characterized protein. We demonstrate that RRP1B physically interacts with a number of nucleosome-binding proteins and transcription factors, all of which have been demonstrated to be potent regulators of gene expression in their own right. Further interaction analyses reveal that RRP1B is associated with markers of heterochromatin and euchromatin, implying that this factor plays a dynamic role in the regulation of gene expression. Finally, we begin to define the functional significance of the rs9306160 non-synonymous *RRP1B* coding polymorphism, which has previously been associated with survival in multiple breast cancer population-based cohorts (14). Specifically, gene expression analyses demonstrate that *RRP1B* allelic variants differentially regulate the expression of a number of transcription factors that are modulated by the RRP1B interactors TRIM28 and DBPA.

EXPERIMENTAL PROCEDURES

Survival Analysis Using the Mvt-1/Rrp1b Microarray Gene Expression Signature—Generation of the Mvt-1/*Rrp1b* gene expression signature has been described elsewhere (14). Briefly, Mvt-1 cells were stably transfected with a mammalian expression vector encoding either full-length mouse *Rrp1b* or *lacZ* as a control. Individual clonal isolates were derived through limiting dilution, and gene expression was quantified using Affymetrix GeneChip Mouse Genome 430 2.0 arrays. To generate a high confidence human transcriptional signature of *Rrp1b* expression, 563 probe sets whose differential expression demonstrated $p < 10^{-4}$ were selected. A gene list representing the probes was developed and used to map to the probe sets of the human U133 Affymetrix GeneChip using the Batch Search function of NetAffx (available on the World Wide Web).

Analysis of tumor gene expression from breast cancer data sets was performed using BRB ArrayTools. Expression data sets were downloaded from the NCBI Gene Expression Omnibus (GEO; available on the World Wide Web; supplemental Table S1). Expression data were loaded into BRB ArrayTools using the Affymetrix GeneChip Probe Level Data option or the Data Import Wizard. Data were filtered to exclude any probe set that was not a component of the *Rrp1b* signature and to eliminate any probe set whose expression variation across the data set was $p > 0.01$. Unsupervised clustering of each data set was performed using the Samples Only clustering option of BRB ArrayTools. Clustering was performed using average linkage, the centered correlation metric, and the Center the Genes analytical option. Samples were assigned into two groups based on the first bifurcation of the cluster dendogram, and Kaplan-Meier survival analysis was performed using the Survival module of the software package Statistica. Significance of survival analyses was performed using the log rank test.

Cell Culture—HEK293 cells were obtained as a gift from Dr. Moon-Kyoo Jang (NIAID, National Institutes of Health, Bethesda, MD). HeLa cells were obtained as a gift from Dr. Chi-Ping Dey (NCI, National Institutes of Health, Bethesda, MD). All cell lines were maintained in Dulbecco's modified Eagle's medium supplemented with 10% fetal bovine serum, 2 mM glutamine, and 100 units of penicillin and streptomycin.

Expression Vectors—Human hemagglutinin (HA)-tagged RRP1B (NCBI accession number BC028386) in the mammalian expression vector pDest-530 was received as a gift from Dr. Doug Lowy (NCI, National Institutes of Health). This vector encodes the wild type 1421C rs9306160 allele. The RRP1B amino-terminal deletion mutant (Δ9–220) and RRP1B central deletion mutant (Δ221–435) were generated by overlap PCR to remove the deletion segment. The carboxyl-terminal deletion (Δ452–749) was generated by partially digesting the wild type HA-*RRP1B* pDest-530 vector with PmlI (New England BioLabs), followed by sequential digestion with MscI (New England BioLabs). Following restriction endonuclease digestion, the remaining fragment was ligated overnight at room temperature using T4 DNA ligase (New England BioLabs). A vector encoding the rs9306160 variant allele (1421T) was generated using the QuikChange XL site-directed mutagenesis system (Stratagene) with the *RRP1B* 1241C pDest-530 vector as a template. The following primers were used for site-directed mutagenesis: 5′-CTTCAGGGCTTTCAGCCCAGAGGCCTC-3′ and 5′-GAGGCCTCTGGGCTGAAAGCCCTGAAG-3′. All vectors were sequence-verified prior to use. *lacZ* pcDNA3.1-V5/His6 (Invitrogen) was used as a control in co-immunoprecipitation experiments.

For tandem affinity purification, the original C-TAP vector, developed for *Schizosaccharomyces pombe*, was a gift from Dr. K. Gould (Vanderbilt University). To generate mammalian tandem affinity purification (TAP) tag vectors for the production of COOH-terminal (C-TAP) fusion proteins, the TAP sequences were modified to include a His_6 tag in place of calmodulin. The TAP domain (His6-two TEV protease sites-two IgG binding domains) was amplified by PCR. The PCR product was cloned into pDest-472. Concurrently, an *RRP1B* entry clone was prepared by cloning the gene using the Gateway BP reaction as recommended by the manufacturer (Invitrogen) in pEntr223 entry vector. The clone was sequence-verified. To prepare the *RRP1B* expression clone in the TAP vector, 150 ng of C-TAP pDest-472 vector (destination vector) was mixed with 100 ng of *RRP1B* pEntr223 in 1× Clonase 2 (Invitrogen) buffer containing essential enzymes. Total volume of the reaction was 10 μl. The reaction mix was incubated at 30 °C for 90 min. Ten micrograms of Proteinase K was added and continued to incubate at 37 °C for 15 min. The vector eGFP C-TAP pDest-472 was used as a control in C-TAP experiments.

Transfection of Cells and Preparation of Extracts for C-TAP Analysis—The protocol for C-TAP analysis to define RRP1B protein-protein interactions has been adapted from Gingras *et al.* (18). HEK293 cells were transfected with either *RRP1B* or eGFP C-TAP pDest-472 vectors using Fugene6 (Roche Applied Science). Forty-eight hours post-transfection, culture medium from plates was removed, and cells were lysed with ice cold lysis III solution (50 mM Tris-Cl, pH 7.5, 150 mm NaCl, 1 mM EDTA,

1% Nonidet P-40, 15% glycerol). Lysates were then frozen on dry ice and defrosted at room temperature. This procedure was repeated an additional two times. Fifteen milliliters of crude cell lysate was poured onto a glass homogenizer receiver placed on wet ice. A Teflon insert was used to further disaggregate cell debris by pressing up and down ~20 times. Cell lysate was transferred to a 15-ml Falcon tube and spun at 3,000 rpm at 4 °C for 5 min.

TAP Tag Purification—Prepared lysates were first subjected to IgG column purification using a disposable 10-ml spin column containing 500 μl of IgG-Sepharose 6-Fast flow resin (Amersham Biosciences). The column was equilibrated according to the manufacturer's protocol. Following equilibration, cell lysates were applied to the column and agitated slowly for thorough mixing at 4 °C for 3–4 h. Following incubation, flow-through was discarded, and beads were washed three times with 10 ml of TST buffer (50 mM Tris-Cl, pH 7.5, 150 mM NaCl, 0.005% Tween 20) for 5 min at 4 °C. After a final wash with TST buffer, columns were equilibrated with 5 ml of TEV protease buffer (10 mM HEPES-KOH, pH 8, 150 mM NaCl, 0.1% Nonidet P-40, 1 mM dithiothreitol), and columns were drained to remove excess buffer, followed by the addition of 1 ml of streptomycin-tagged TEV protease (50 μg). Columns were then incubated at 4 °C with agitation overnight. Columns were then placed inside a 50-ml tube and spun for 30 s at 500 rpm to recover tapped protein after TEV digestion.

Eluted proteins were then subjected to a second round of purification using nickel-Sepharose high performance resin (GE Healthcare), which was conditioned for binding of His-tagged proteins according to the manufacturer's protocol. One milliliter of conditioned nickel-resin was added to 750 μl of sample in a total volume 2 ml, with the excess volume being made up of TCB buffer. The contents were incubated at 4 °C for 30 min, the flow-through was discarded, and the column was washed with 10 ml of TCB buffer on a rotary shaker for 15 min at 4 °C. The washing step was repeated twice. First elution was done by adding 400 μl of TCB containing 500 mM imidazole. Samples were incubated for 10 min, and eluant was collected. This elution step was repeated twice using TCB containing 1 M immidazole. The three elution volumes were combined and analyzed using PAGE.

Trypsin Digest and Preparation of C-TAP Samples for Mass Spectrometry—One microgram of sequencing grade modified trypsin (Promega) was added directly to the eluate, and digestion was performed overnight at 37 °C. Following digestion, the sample was lyophilized and resuspended in reversed-phase HPLC buffer A (20 μl; 0.4% AcOH, 0.005% heptafluorobutyric anhydride in H_2O). Prior to loading onto the reversed phase column, the sample was centrifuged at 13,000 rpm for 10 min, and the supernatant was transferred to a fresh tube.

Liquid Chromatography-MS/MS—Microcapillary reversed-phase columns (75-μm inner diameter, 363-μm outer diameter; Polymicro Technology) were cut to a final length of 15–20 cm, and spray tips were pulled in-house by hand. Columns were packed in-house (12 cm) with Magic C18 100-Å, 5-μm silica particles (Michrom) using a pressure bomb. Prior to loading the sample, columns were equilibrated in HPLC buffer A. Half of the sample was applied to the column using a pressure bomb and then washed off line in buffer A and 5% acetonitrile for 30–60 min. The liquid chromatography column was then placed in front of a Finnigan LCQ mass spectrometer, programmed for data-dependent MS/MS acquisition (one survey scan, three MS/MS of the most abundant ions). After sequencing the same species three times, the mass ± 3 Da was placed on an exclusion list for 3 min. Peptides were eluted from the reversed-phase column using a multiphasic elution gradient (5–14% acetonitrile over 5 min, 14–40% over 60 min, and 40–80% over 10 min). The remaining half of the sample was then processed in the same manner. To prevent cross-contamination, each sample was processed on a freshly prepared reversed-phase column. Liquid chromatography/MS-MS data were analyzed by generating raw files using Xcalibur (Finnigan), which were subsequently converted to the mzXML format. Combined runs (from the same sample) were searched using SEQUEST against the human International Protein Index data base.

Transfections and Lysate Preparation for Co-Immunoprecipitation—For co-immunoprecipitation (co-IP), HEK293 cells were transfected with one of the following vectors: HA-RRP1B pDest-530, HA-RRP1B pDest-530 Δ9–220, HA-RRP1B pDest-530 Δ452–749, or pcDNA3.1 *lacZ* V5-His6. Supercoiled plasmids were transfected using Superfect Transfection Reagent (Qiagen, Valencia, CA) as per the manufacturer's instructions. Briefly, transfections were performed in 100-mm diameter culture dishes, with 2×10^6 HEK293 cells being seeded 24 h prior to transfection. Cells in each culture vessel were transfected with a total of 10 μg of vector DNA using Superfect at a 6:1 lipid/DNA ratio. Two days after transfection, cells were lysed with 200 μl of ice-cold chromatin extraction buffer (CEB; 300 mM NaCl, 100 nM EGTA, 20 mM Tris-HCl, pH 7.4, 2 mM $MgCl_2$, 1% Triton X-100, 1× Complete Mini EDTA-free protease inhibitor (Roche Applied Science)), and lysates were stored at −80 °C until use.

Transfections and Total RNA Preparation for Quantitative Real Time PCR—For quantitative real time PCR (qPCR), HeLa cells were transfected with one of the following vectors: HA-RRP1B 1421C pDest-530, HA-RRP1B 1421T pDest-530, or pcDNA3.1 *lacZ* V5-His6. Transfections were performed in triplicate in 6-well plates, with 4×10^5 HeLa cells being seeded 24 h prior to transfection. Cells in each culture vessel were transfected with a total of 2 μg of vector DNA using Superfect at a 6:1 lipid to DNA ratio. Total RNA was isolated from cell culture samples using an RNeasy Mini Kit (Qiagen) with on-plate lysis using buffer RLT. Sample homogenization was performed by vigorous pipetting. All samples were subjected to on-column DNase digestion.

Co-immunoprecipitation—Interactions with RRP1B detected on TAP analysis were confirmed by co-IP using GammaBind Sepharose-G beads (Roche Applied Science). Prior to co-IP, beads were prepared by washing 200 μl of 50% bead slurry with 1 ml of CEB, followed by aspiration of excess CEB and the addition of 100 μl of CEB to reform a 50% bead slurry. Lysate from one 100-mm plate was then precleared by rotation at 4 °C for 15 min using 40 μl of 50% bead slurry. Following incubation, the beads were pelleted by centrifugation at 10,000 rpm at 4 °C, and the supernatant was transferred to a fresh tube. RRP1B-anti-

body complexes were formed by rotating precleared lysates for 1 h at 4 °C with 10 μg of high affinity anti-HA antibody (catalog number 11 867 423 001; Roche Applied Science). Following this, 50 μl of 50% bead slurry was added to each sample, and samples were rotated overnight at 4 °C. Subsequently, beads were pelleted by centrifugation at 10,000 rpm at 4 °C, the supernatant was discarded, and beads were washed with 1 ml of CEB. The wash step was repeated a total of three times. Twenty-five microliters of 2× Laemmli sample was then added, and samples were boiled for 10 min and centrifuged at full speed for 5 min.

To define interactions between endogenous RRP1B and its potential binding partners, immunoprecipitations were performed as above, using lysate harvested from untransfected HEK293 cells. Immunoprecipitation of RRP1B was performed using 2 μg/ml anti-NNP-1B (K-19) (catalog number sc-83327; Santa Cruz Biotechnology, Inc., Santa Cruz, CA). As a control, a mock immunoprecipitation was also performed using 2 μg/ml rabbit IgG (Upstate).

Western Blot Analysis of Co-immunoprecipitated RRP1B Interactors—SDS-PAGE was performed for 60–90 min at 120 V using the XCell SureLock™ minicell (Invitrogen). Immunoprecipitated samples and input controls were analyzed using NuPAGE Novex gels (Invitrogen). The gel and buffer used depended upon the molecular weight of the interactor and included 10% bis-tris, 4–12% bis-tris, and 3–8% Tris acetate gels with 1× MOPS, 1× MES, or 1× Tris acetate running buffers (Invitrogen). Proteins were transferred to Immobilon-P membranes (Millipore) and immunoblotted against endogenous RRP1B interactors. One of the following primary antibodies was used for this purpose as per the manufacturer's protocol: anti-CSDA (catalog number ab56374; Abcam), anti-acetyl histone H4 Lys5 (catalog number ab51997; Abcam), anti-histone HIFX (catalog number ab17729; Abcam), anti-HP1α (catalog number 07-346; Millipore), anti-NCL (catalog number ab16940; Abcam), anti-NPM1 (catalog number GTX90863; GenTex), anti-PARP1 (catalog number H00000142-M01; Abnova), and anti-TRIM28 (catalog number ab22553; Abcam). Blots were subsequently stripped with Restore Western blot stripping buffer and reprobed with anti-HA tag (Roche Applied Science).

Co-Immunofluorescence—For co-immunofluorescence, HeLa cells were transfected with one of the following vectors: HA-RRP1B pDest-530, HA-RRP1B pDest-530 Δ9-220, HA-RRP1B pDest-530 (Δ221–435), or HA-RRP1B pDest-530 Δ452-749. Supercoiled plasmids were transfected using Superfect transfection reagent (Qiagen, Valencia, CA) as per the manufacturer's instructions. Briefly, transfections were performed in 2-well glass chamber slides (Nunc), with 1×10^5 HeLa cells being seeded 24 h prior to transfection. Cells in each culture vessel were transfected with a total of 1 μg of vector DNA using Superfect at a 6:1 lipid/DNA ratio. Twenty-four hours after transfection, cells were washed with 1× PBS, fixed for 15 min at room temperature with Histochoice MB Fixative® (Electron Microscopy Services), and permeabilized with 0.2% Triton X-100 in 1× PBS for 15 min at room temperature. Samples were then blocked with 5% bovine serum albumin and incubated with the primary antibody at room temperature for 1 h. In addition to those antibodies listed above for immunoblot analysis, the following antibodies were utilized for co-immunofluorescence: anti-histone H3 trimethyl-Lys9 (catalog number 07-442; Millipore), anti-histone H3 dimethyl-Lys27 (catalog number ab24684; Abcam), and anti-LMNB1 (catalog number ab16048; Abcam). All antibodies were used as per the manufacturer's protocol. Following primary antibody incubation, slides were washed three times with 1× PBS, and secondary antibody incubation was performed as per the manufacturer's protocol. Secondary antibodies were purchased from Invitrogen (Alexa Fluor® 594 goat anti-rat (catalog number A11007), Alexa Fluor® 594 goat anti-rabbit highly cross-adsorbed (catalog number A11037), Alexa Fluor® 594 goat anti-mouse highly cross-adsorbed (catalog number A11032), Alexa Fluor® 488 goat anti-mouse highly cross-adsorbed (catalog number A11029)) and BD Biosciences (fluorescein isothiocyanate goat anti-rabbit (catalog number 554020)). Slides were washed three times with 1× PBS and mounted with Vectashield with DAPI (Vector Laboratories), and confocal microscopy was performed using a ×63 objective. Measurements of maximum nuclear diameters were performed using LSM 5 Image Browser (Zeiss).

Nuclear Matrix Preparation—Sequential nuclear extractions were performed as described (19). Briefly, HeLa cells were seeded in 2-well chamber slides and transfected with the HA-*RRP1B* pDest-530 vector as described above. One day after transfection, cells were washed with PBS at 4 °C and incubated for 10 min in ice-cold cytoskeleton buffer (10 mM NaCl, 300 mM sucrose, 10 mM PIPES, pH 6.8, 3 mM $MgCl_2$, 0.5% Triton X-100, 1× Halt protease inhibitor mixture (Pierce), 20 units/ml recombinant RNasin (Promega) ribonuclease inhibitor). Cells were then incubated in extraction buffer (250 mM ammonium sulfate, 300 mM sucrose, 10 mM PIPES, pH 6.8, 3 mM $MgCl_2$, 0.5% Triton X-100, 1× Halt protease inhibitor mixture (Pierce), 20 units/ml recombinant RNasin (Promega)) on ice for 5 min. Finally, cells incubated with digestion buffer (50 mM NaCl, 300 mM sucrose, 10 mM PIPES, pH 6.8, 3 mM $MgCl_2$, 0.5% Triton X-100, 1× Halt protease inhibitor mixture (Pierce), 20 units/ml recombinant RNasin (Promega) ribonuclease inhibitor, 500 units/ml RQ1 RNase-free DNase (Promega)) at 37 °C for 4 h. After each step, one chamber slide was removed, and cells were fixed with Histochoice as described above.

Quantitative Real Time PCR Gene Expression Analysis—cDNA was synthesized from RNA isolated from transfected cell lines using the iScript reverse transcription-PCR System (Bio-Rad) by following the manufacturer's protocol. Single reverse transcription-PCRs were performed for each replicate transfection. qPCR was performed to detect the cDNA levels of *RRP1B* and a number of transcripts previously shown to be regulated by either TRIM28 or CSDA using an ABI 7900HT sequence detection system. *RRP1B* ectopic expression was confirmed using an *RRP1B*-specific TaqMan probe (Applied Biosystems Assay on Demand Hs00380154_m1), with expression being normalized to *GUSB* (β-glucuronidase) (Applied Biosystems). Reactions were carried out in duplicate using Universal PCR Mastermix (Applied Biosystems) as per the manufacturer's protocol. All other reactions were performed in duplicate using QuantiTect SYBR Green master mix (Qiagen) as per the manufacturer's protocol. The cDNA level of each gene was normalized to *GUSB* cDNA levels using custom-designed primers for

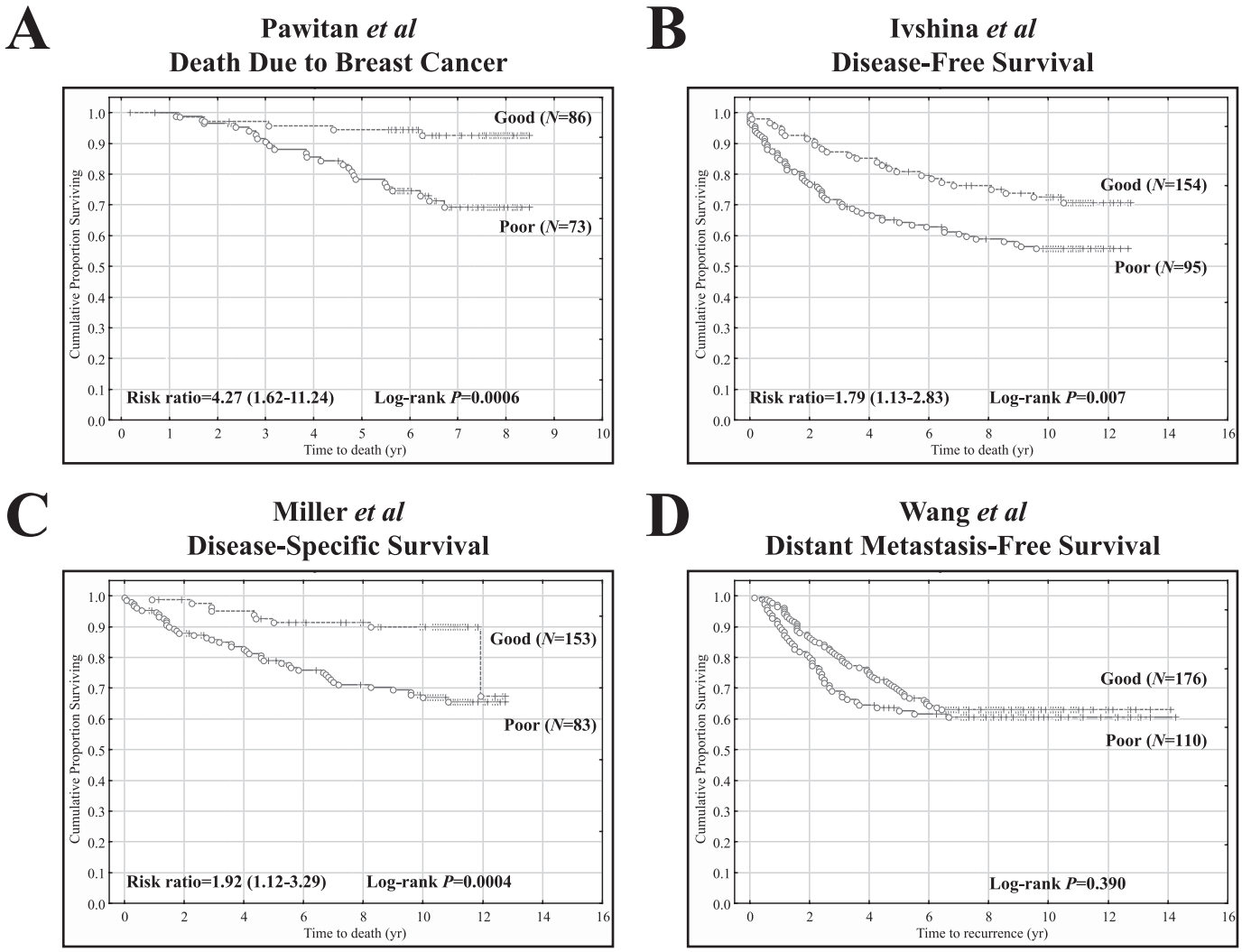

FIGURE 1. **The *Rrp1b* activation signature predicts the risk of survival but not relapse in multiple breast cancer data sets.** *A*, a significant difference in the overall likelihood of survival was observed in the Pawitan *et al.* (20) data set, with 8-year survival being 92% *versus* 69% for the good and poor prognosis *Rrp1b* signatures, respectively. *B*, 12-year disease-free survival was 71% *versus* 56% in the Ivshina *et al.* (22) data set for the good and poor prognosis *Rrp1b* signatures, respectively. *C*, a similar effect was observed in the Miller *et al.* (21) data set with 12-year survival being 90% *versus* 65% for the good and poor prognosis *Rrp1b* signatures, respectively. *D*, the Wang *et al.* (23) data set differs in that the study end point is local or distant disease recurrence rather than patient death. No survival effect was observed with *Rrp1b* signature gene survival in this data set.

SYBR green-amplified target genes (supplemental Table S2). Target transcripts were quantified using the relative standard curve method. Differences in target expression were determined by comparing the relative transcript quantity in individual *RRP1B* variant allele transfections with the average relative transcript quantities in *lac*Z transfections. Significance levels for comparisons were performed using the Mann-Whitney *U* test, with relative quantities of *RRP1B*-transfected and *lac*Z-transfected HeLa cells used for analyses.

RESULTS

The Rrp1b Activation Signature Predicts Survival in Multiple Breast Cancer Data Sets—Our earlier study involved stably expressing full-length mouse *Rrp1b* in the highly metastatic Mvt-1 mouse mammary tumor cell line, followed by analysis of cellular gene expression patterns using Affymetrix microarrays (14). A high confidence human *Rrp1b* gene expression signature was generated by mapping the most significantly differentially regulated genes ($p < 10^{-4}$) from mouse array data to human Affymetrix probe set annotations. For each of the four data sets, the resulting gene signature consequently varied from 202 to 302 probe sets (supplemental Table S1). Human *Rrp1b* profiles were then used for unsupervised clustering of publicly available data sets into two groups representing high and low levels of *Rrp1b* activation in patient samples. Kaplan-Meier survival analysis was then performed to investigate whether there was a survival difference between the two groups. *Rrp1b* signature gene expression accurately predicted outcome in three of the four breast cancer data sets (those from Pawitan *et al.* (20), Miller *et al.* (21), and Ivshina *et al.* (22); Fig. 1). The end point for these studies was disease-free survival, as opposed to in Wang *et al.* (23), where the end point was distant metastasis-free survival. Characterization of *Rrp1b* signature genes associated with survival in each of the breast cancer data sets revealed overlapping but not identical gene expression signatures (supple-

TABLE 1
Proteins interacting with RRP1B on tandem affinity purification analysis

Gene symbol	Description	Accession number	Number of interactions detected with		
			Control	Human	Mouse
C1QBP	Complement component 1 Q subcomponent-binding protein, mitochondrial precursor	Q07021			4
C21orf30	Putative uncharacterized protein	Q9UFM2			2
CDCA8	Cell division cycle-associated protein 8 (Borealin)	Q53HL2			3
CROP	Cisplatin resistance-associated overexpressed protein (Luc7A)	O95232		1	3
CSDA	Cold shock domain-containing protein A	P16989		1	10
CUBN	Cubilin precursor	O60494		2	3
DDX21	DEAD box protein 2 (nucleolar RNA helicase II)	Q9NR30		2	3
DDX47	Probable ATP-dependent RNA helicase DDX47 (DEAD box protein 47)	Q9H0S4			3
DKFZp686E23209	Hypothetical protein DKFZp686E23209	Q68CN4	1		5
DNAJC9	DnaJ homolog subfamily C member 9	Q8WXX5			2
ERH	Enhancer of rudimentary homolog	P84090			2
GARNL1	GTPase-activating Rap/Ran-GAP domain-like 1	Q6GYQ0			2
H1FX	Histone H1x	Q92522		3	3
HNRNPA1	Heterogeneous nuclear ribonucleoprotein A1	P09651	1	6	12
HNRPUL1	Heterogeneous nuclear ribonucleoprotein U-like protein 1	Q9BUJ2			3
IGKC	Immunoglobulin κ constant	Q569I9		3	1
IGKV2–40	Ig κ chain V-II region	P01614		3	3
ILF3	Interleukin enhancer-binding factor 3 (nuclear factor of activated T-cells 90 kDa)	Q12906		2	5
ITGAD	Integrin α-D precursor (CD11d antigen)	Q13349			2
LARP1	La ribonucleoprotein domain family member 1	Q6PKG0		3	
LRRC59	Leucine-rich repeat-containing protein 59	Q96AG4			4
LUC7L2	Putative RNA-binding protein Luc7-like 2	Q9Y383		1	5
LYAR	Ly1 antibody-reactive homolog	Q9NX58			2
MAP3K7IP1	Mitogen-activated protein kinase kinase kinase 7-interacting protein 1 (TGF-β-activated kinase 1-binding protein)	Q15750			2
MKI67	Antigen KI-67	P46013			2
NCL	Nucleolin	P19338	1	23	22
NEDD1	Neural precursor cell-expressed, developmentally down-regulated 1	Q8NHV4			2
NPM1	Nucleophosmin (B23)	P06748	2	12	18
PARP1	Poly(ADP-ribose) polymerase 1	P09874		2	6
PPP1CA	Serine/threonine-protein phosphatase PP1-α catalytic subunit	P62136		2	4
PRKAR1A	cAMP-dependent protein kinase type I-α regulatory subunit	P10644			2
PRPF4B	Serine/threonine-protein kinase PRP4 homolog	Q13523		1	3
RCN1	Reticulocalbin-1 precursor	Q15293			4
RPL10A	60 S ribosomal protein L10a	P62906		3	3
RPL4	60 S ribosomal protein L4	P36578		4	4
RPL5	60 S ribosomal protein L5	P46777		8	5
RPLP0	60 S acidic ribosomal protein P0	P05388		4	2
RRP1B	Ribosomal RNA processing 1 homolog B	Q14684		15	16
RSL1D1	Ribosomal L1 domain-containing protein 1	O76021		2	3
SDF2L1	Dihydropyrimidinase-like 2	Q86U75		2	
SFRS1	Splicing factor, arginine/serine-rich 1 (pre-mRNA-splicing factor SF2, P33 subunit)	Q07955		2	4
SFRS6	Splicing factor, arginine/serine-rich 6 (pre-mRNA-splicing factor SRP55)	Q13247		2	4
SLC22A11	Solute carrier family 22 member 11 (organic anion transporter 4)	Q9NSA0		3	
SRP14	Signal recognition particle 14-kDa protein	P37108			2
STAU1	Staufen homolog 1	O95793			3
THOC4	THO complex subunit 4	Q86V81		1	3
TOP1	DNA topoisomerase I	P11387		2	
TRIM28	Tripartite motif-containing protein 28 (transcription intermediary factor 1-β)	Q13263			3
YY2	YY2 transcription factor	O15391			2

mental Table S3). The directionality of hazard ratios was consistent when a probe set was predictive of survival in more than one cohort in all instances. Finally, the *Rrp1b* signature was the only consistent predictor of outcome on multivariate Cox proportional analysis in all of the cohorts (supplemental Table S4). Given all of these observations, we therefore argue that the net effect of the *Rrp1b* signature is both consistent and robust.

Analysis of RRP1B Protein-Protein Interactions—To gain a better understanding of the functional activity of RRP1B, interacting proteins were defined using TAP analysis. The identities of proteins putatively interacting with the mouse and human homologs of RRP1B are shown in Table 1. It can be seen from these data that RRP1B potentially interacts with a wide variety of proteins including an abundance of RNA-binding proteins, implying that RRP1B plays a prominent role in RNA metabolism. Gene ontological analysis was performed using GeneInfoViz (24) to determine whether any commonality in biological function existed between the large number of RRP1B interactors identified. Results from gene ontological analysis are

shown in supplemental Fig. S1 and demonstrate that RRP1B interacts with factors proven to be involved in a wide variety of biological processes, including, but not limited to, regulation of cellular proliferation and the cell cycle, regulation of transcription, ribosome biogenesis, and mRNA splicing.

Characteristics of Ectopically Expressed RRP1B in Interphase Cells—Previous studies (25) and the finding that RRP1B binds various nucleolar proteins in TAP analysis (*e.g.* NCL (nucleolin) and NPM1 (nucleophosmin)) suggest that RRP1B might localize to the nucleolus. To confirm this, co-immunofluorescence (co-IF) was performed in HeLa cells for ectopically expressed HA-tagged RRP1B and the endogenous nucleolar marker, fibrillarin. Ectopically expressed RRP1B was utilized since we do not have an endogenous RRP1B antibody that can be used for IF. Co-IF demonstrated that RRP1B is a perinucleolar protein that co-localizes with fibrillarin in the perinucleolar region (Fig. 2*A*, *upper panels*). These initial experiments also demonstrated that RRP1B localizes to the nuclear periphery, which was confirmed by co-staining cells for ectopic RRP1B and the endogenous nuclear envelope matrix protein lamin B1 (Fig. 2*A*, *lower panels*). Furthermore, measurements of nuclear diameters reveal that ectopic expression of *RRP1B* increases nuclear diameter (supplemental Fig. S2). Specifically, the average maximum nuclear diameter of *RRP1B*-transfected HEK293 cells was 17.97 $\pm$ 2.49 μm compared with 15.05 $\pm$ 2.37 μm for untransfected HEK293 cells ($p = 0.001$) and 18.16 $\pm$ 2.76 μm for HeLa cells transfected with *RRP1B* compared with 15.91 $\pm$ 2.55 μm for untransfected HeLa cells ($p = 0.018$).

Analysis of RRP1B Nuclear Localization Signals—RRP1B contains only one known protein domain, an NH_2-terminal RNA-binding Nop52 domain (pfam05997). This amino terminus motif bears significant structural homology to the *Saccharomyces cerevisiae* ribosomal RNA processing factor RRP1, which is involved in the biogenesis of 60 S ribosomal subunits (26). *In silico* analysis of RRP1B structure using PredictNLS (27), however, reveals that the relatively disordered carboxyl half of this protein contains three nuclear localization signals (*NLS* in Fig. 2*B*; see supplemental material). Therefore, to investigate the role that these domains, as well as the amino terminus Nop52 domain, plays in cellular localization, various RRP1B deletion mutants were constructed (Fig. 2*B*), and the subcellular localization was determined by immunofluorescence (Fig. 2*C*). Deletion of the Nop52 ribosomal RNA processing domain had the least effect, with the RRP1B mutant protein still localizing to the perinuclear and perinucleolar regions of the nucleus (Fig. 2*C*, *left*). However, ectopic expression of the ΔNop52 deletion mutant did induce the presence of misshapen nucleoli and also a degree of cytoplasmic signal, especially surrounding the nuclear envelope. Deletion of the central portion of RRP1B, which contains NLS1, appears to ablate localization of RRP1B to the nuclear periphery (Fig. 2*C*, *middle*). Ectopic expression of the carboxyl terminus deletion mutant that lacks NLS2 and -3 resulted in diffuse RRP1B staining throughout the cytoplasm and nucleus, with a strong signal only observed at the nuclear periphery (Fig. 2*C*, *left*).

Confirmation of Putative Protein-Protein Interactions—Given the previously described profound effects of *Rrp1b* dysregulation upon global patterns of gene expression (14), we chose to focus upon confirming the interactions between RRP1B and transcriptional regulators (*e.g.* TRIM28 (tripartite motif-containing 28) and CSDA (cold shock domain protein A)) and factors that have been shown to modulate chromatin structure (*e.g.* PARP1 (poly(ADP-ribose) polymerase 1), H1X (H1 histone family member X), NCL, and NPM1). Interactions were confirmed by ectopically expressing RRP1B in either the HEK293 or HeLa cells and performing co-IP and co-IF to detect RRP1B binding with the endogenous interactor. Co-IP confirmed that ectopically expressed RRP1B does indeed physically interact with the endogenous forms of all of these modulators of transcription and chromatin structure (Fig. 3*A*). Furthermore, these interactions with the endogenous proteins appear to occur with the carboxyl terminus of RRP1B in all cases apart from PARP1, which interacts with the amino terminus Nop52 domain of RRP1B. We do, however, acknowledge that the interaction with PARP1 is relatively weak. However, it is highly unlikely that the RRP1B-PARP1 interaction is an experimental artifact, since there is loss of binding with the ΔC-term sample. Co-IF analyses supported these interactions by demonstrating co-localization between ectopic RRP1B and its endogenous interactor (Fig. 3*B*). RRP1B and its interactors appear to co-localize at the perinuclear or perinucleolar regions, within the nucleoplasm, or at a combination of any of the three.

Further experiments were performed to confirm that these interactions were not an artifact of ectopically expressing *RRP1B*. Specifically, we defined interactions between endogenous RRP1B and several of the potential interactors described above in untransfected HEK293 cells. We were able to confirm all of the interactions tested in this manner (supplemental Fig. S3).

RRP1B Is Associated with Chromatin during Mitosis—Unexpectedly, during the co-IF experiments, confocal microscopy of HeLa cells demonstrated an association of RRP1B with condensed mitotic chromatin (Fig. 4). The NH_2 terminus ΔNop52 and ΔCOOH terminus deletion mutants also were observed in association with condensed mitotic chromatin. In contrast, the ΔMid RRP1B deletion mutant shows no co-localization with metaphase chromatin, again implying the importance of this region in the functional activity of RRP1B. This is an intriguing observation, since there is significant interspecies sequence divergence in the central portion of RRP1B. For example, there is less than 40% homology between the central thirds of human and mouse RRP1B proteins (see supplemental material).

RRP1B Is Associated with both Heterochromatin and Euchromatin—Given the apparent association of RRP1B with mitotic chromosomes by confocal microscopy (Fig. 4) as well as its apparent interaction with several regulators of transcription and chromatin structure, we proceeded to investigate whether RRP1B interacts with markers of heterochromatin and euchromatin. Indirect immunofluorescence microscopy was used to monitor the effect of sequential treatment of *RRP1B* transfected with Triton X-100, ammonium sulfate, and DNase on the localization of RRP1B (Fig. 5*A*). These experiments reveal that RRP1B is resistant to extraction, confirming the DNA binding properties of this protein. DNase digestion was confirmed by DAPI staining and revealed that nuclear RRP1B is also partially associated with the nuclear matrix (Fig. 5*A*, *bot-*

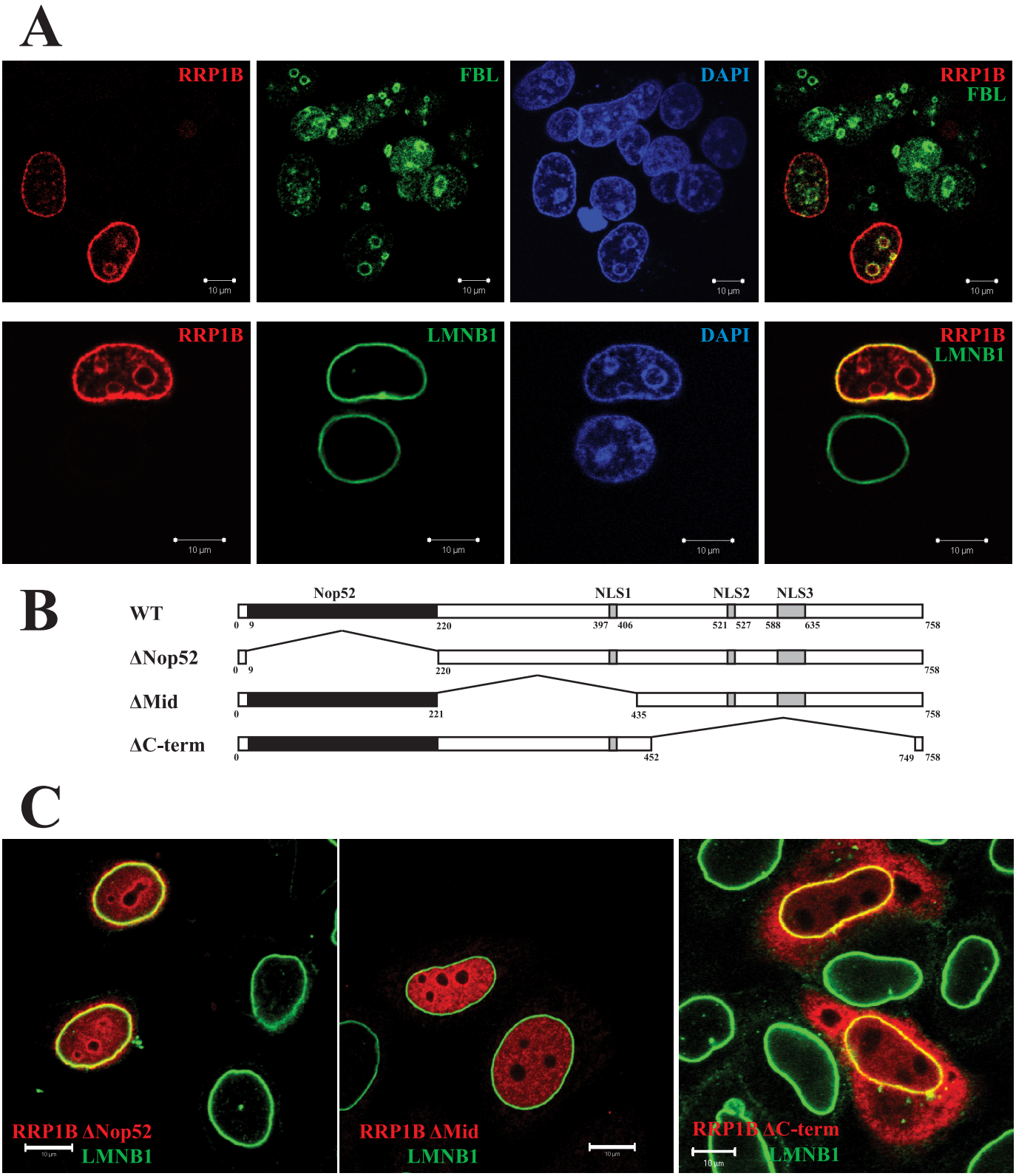

FIGURE 2. **Characteristics of cells ectopically expressing RRP1B.** *A*, co-IF followed by confocal microscopy was performed to define the cellular localization of RRP1B. Hemagglutinin-tagged, full-length RRP1B was ectopically expressed in HeLa cells to define its cellular localization. Cells were co-stained for ectopic RRP1B (*red*), either the nucleolar marker fibrillarin (*FBL*; *top*) or the nuclear envelope marker lamin B1 (*LMNB1*; *bottom*) (*green*), and double-stranded DNA (*DAPI*; *blue*). *B*, comparison of the structures of the full-length RRP1B (*WT*) with that of the amino terminus (Δ*Nop52*), central (Δ*Mid*), and carboxyl terminus (Δ*C-term*) deletion mutants. *C*, cellular localizations of the three deletion mutants in relation to that of the nuclear envelope protein, LMNB1. *Bar*, 10 μm.

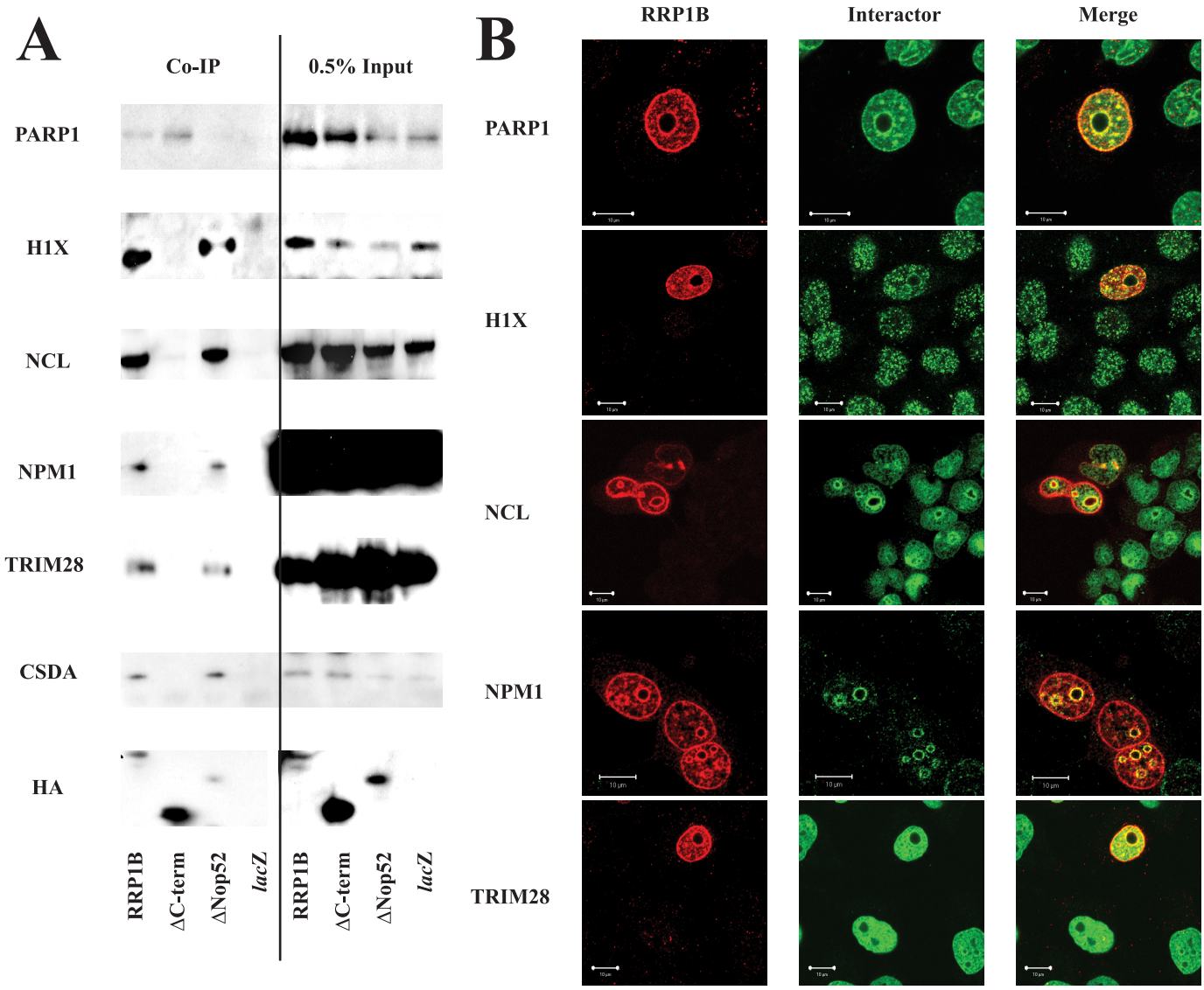

FIGURE 3. **RRP1B interacts with various nucleosome-associated proteins.** *A*, following TAP analysis to screen for RRP1B binding partners, co-IP was performed to confirm interactions between RRP1B and nucleosome-associated proteins. HEK293 cells were transiently transfected with either the full-length RRP1B transcript (*WT*) or the amino terminus (Δ*Nop52*) or carboxyl terminus (Δ*C-term*) deletion mutants. Following immunoprecipitation, interactions were defined by blotting for the endogenous binding partner. *B*, indirect immunofluorescence was performed to confirm the interaction of RRP1B with these nucleosome binding proteins. HeLa cells were co-stained for ectopically expressed full-length RRP1B (*red*) and the endogenous interactor (*green*), and localization was confirmed using confocal microscopy. *Bar*, 10 μm.

tom). To further investigate the association of RRP1B with chromatin, co-IPs were performed with a number of chromatin-associated factors. These revealed that RRP1B physically interacts with HP1α (heterochromatin protein 1α) (Fig. 5*B*), the potent inducer of heterochromatinization and gene silencing. Co-localization of RRP1B and HP1α is evident upon co-IF analysis, primarily at punctate loci throughout the nucleus (Fig. 5*C*, *upper panels*). Interestingly, when compared with untransfected cells in the same experiment, ectopic expression of RRP1B appears to redistribute HP1α throughout the nucleus, with RRP1B transfectants displaying stronger HP1α staining at the perinuclear and perinucleolar regions (Fig. 5*C*, *upper panels*, *green channel*; untransfected cells are seen *below* the RRP1B-expressing cells). In addition to a physical interaction with HP1α, we also demonstrate that RRP1B co-localizes with a several histone markers of heterochromatin, including histone H3 trimethyl-lysine 9 (H3K9me3) and histone H3 dimethyl-lysine 27 (H3K27me2). However, co-IP analysis did not reveal a physical interaction between RRP1B and these heterochromatin markers (data not shown).

As mentioned above, dysregulation of either RRP1B or BRD4 appears to have similar effects upon tumor progression and metastasis as well as upon global patterns of gene expression (14, 17). Additionally, both physically interact with the previously described metastasis efficiency modifier SIPA1 (14, 16). It has previously been demonstrated that BRD4 binds to acetylated histones (acetyl histone H3 lysine 14 (AcH3K14), acetyl histone H4 lysine 5 (AcH4K5), acetyl histone H4 lysine 12 (AcH4K12)) (28). This binding of BRD4 to acetylated histones induces positive transcription elongation factor b (P-TEFb) complex recruitment to target promoters, phosphorylation of RNA polymerase II, and subse-

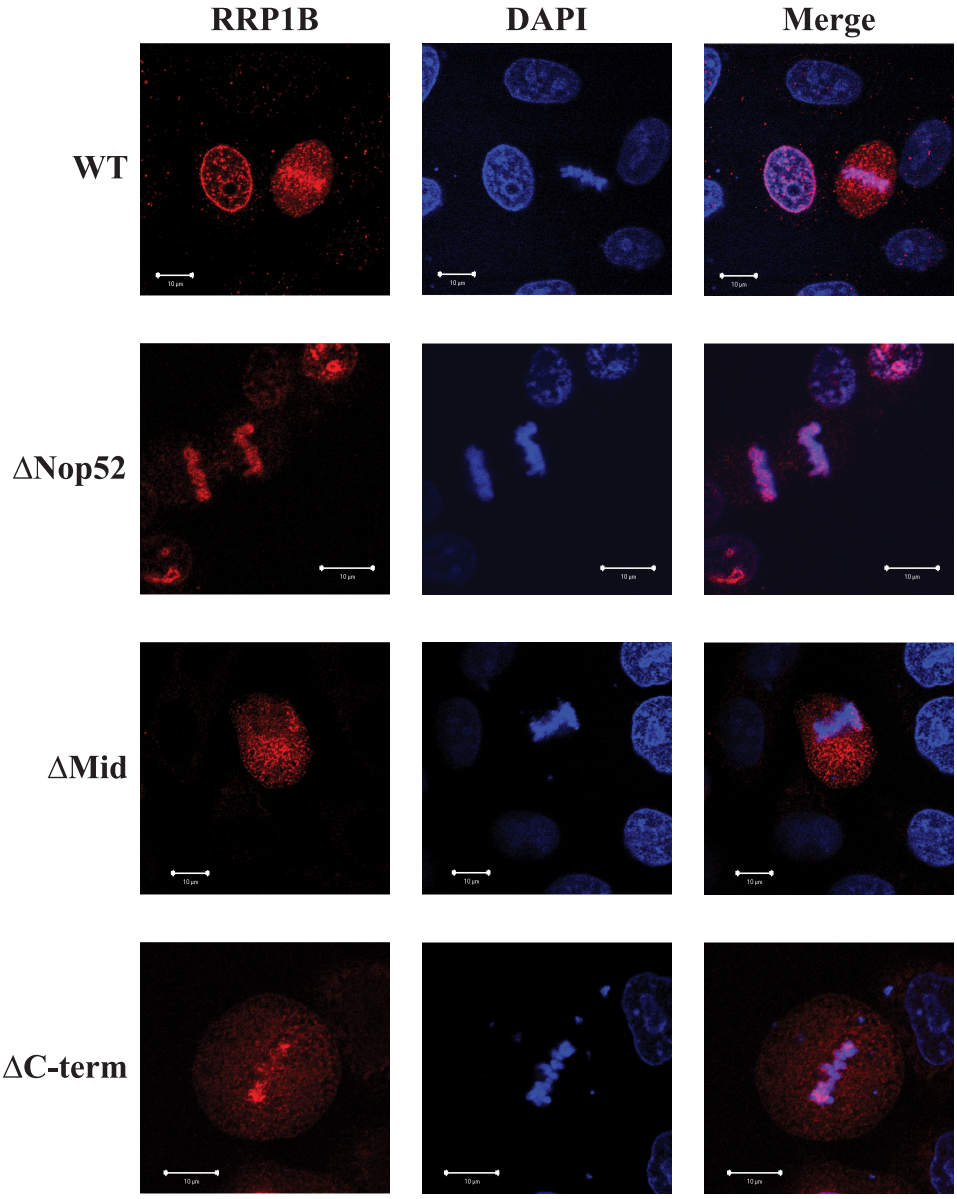

FIGURE 4. **Localization of full-length RRP1B and RRP1B deletion mutants during mitosis.** HeLa cells were transiently transfected with either the full-length RRP1B transcript (*WT*) or the amino terminus (Δ*Nop52*), central (Δ*Mid*) and carboxyl terminus (Δ*C-term*) deletion mutants. Immunofluorescence followed by confocal microscopy was performed by staining for the ectopically expressed protein (*red*) and double-stranded DNA (*DAPI*; *blue*). *Bar*, 10 μm.

quent transcriptional elongation (29). Given the apparent functional relationship between RRP1B and BRD4, we therefore investigated whether RRP1B interacts with various forms of the acetylated histone bound by BRD4. Co-IP revealed that the carboxyl terminus of RRP1B interacts with AcH4K5 (Fig. 5*B*) but not with AcH3K14, AcH4K12, components of the P-TEFb complex, or BRD4 itself (data not shown). Co-IF demonstrates that RRP1B appears to co-localize with AcH4K5 throughout the nucleus but primarily at the perinuclear and perinucleolar regions of RRP1B-transfected cells (Fig. 5*C*). Finally, co-IF demonstrates that RRP1B and BRD4 do not co-localize with one another, implying that a physical interaction between these two proteins is unlikely (Fig. 5*C*).

Expression Analysis of TRIM28- and CSDA-regulated Transcripts—Recent studies have defined transcripts regulated by a number of transcription factors that physically interact with RRP1B. We therefore tested the effect of transient *RRP1B* ectopic expression upon the expression levels of TRIM28-regulated transcripts (*ZNF333*, *ZNF426*, *ZNF433*, and *ZNF554* (30)) and CSDA-regulated transcripts (*ASCL1*, *CTSL*, *CA3*, *DNAJC12*, *HPX*, and *ORM2* (31)) in HeLa cells. Our earlier work demonstrated that the variant allele, the rs9306160 (1421C→T) single nucleotide polymorphism, which encodes a proline to leucine substitution within RRP1B, is associated with improved survival in multiple breast cancer cohorts (14). We therefore chose to quantify whether ectopic expression of either allelic variant had differential effects upon TRIM28- and CSDA-regulated targets. Following reverse transcription-PCR, qPCR demonstrated that the ratio of *RRP1B* expression in cells transfected with the wild type 1421C allele compared with *lacZ*-transfected cells was 5.83 ± 0.63 ($p < 0.05$; supplemental Table S5). The ratio of *RRP1B* expression in cells transfected with the variant 1421T allele compared with *lacZ*-transfected cells was 5.90 ± 0.23 ($p < 0.05$; supplemental Table S5). With regard to the TRIM28-regulated transcripts, all but ZNF433 were expressed in HeLa cells. All of the expressed Krüppel-associated box (KRAB)-zinc finger (ZNF) transcription factors were significantly down-regulated by ectopic expression of the wild type 1421C *RRP1B* allele (Fig. 6*A*). However, only *ZNF554* was significantly down-regulated by the 1421T variant *RRP1B* allele, suggesting that the wild type and variant *RRP1B* alleles differentially regulate *ZNF333* and *ZNF426*. The CSDA-regulated transcripts *CA3* and *ORM2* are not expressed in HeLa cells. Of the four remaining transcripts, *ASCL1* and *DNAJC12* were down-regulated, and HPX was up-regulated by ectopic expression of the wild type 1421C *RRP1B* allele (Fig. 6*B*). A similar effect upon the expression levels of *DNAJC12* and *HPX* was observed with ectopic expression of the variant 1421T *RRP1B* allele. However, the expression levels of *ASCL1* were not significantly down-regulated by the 1421T variant allele, which again suggests that

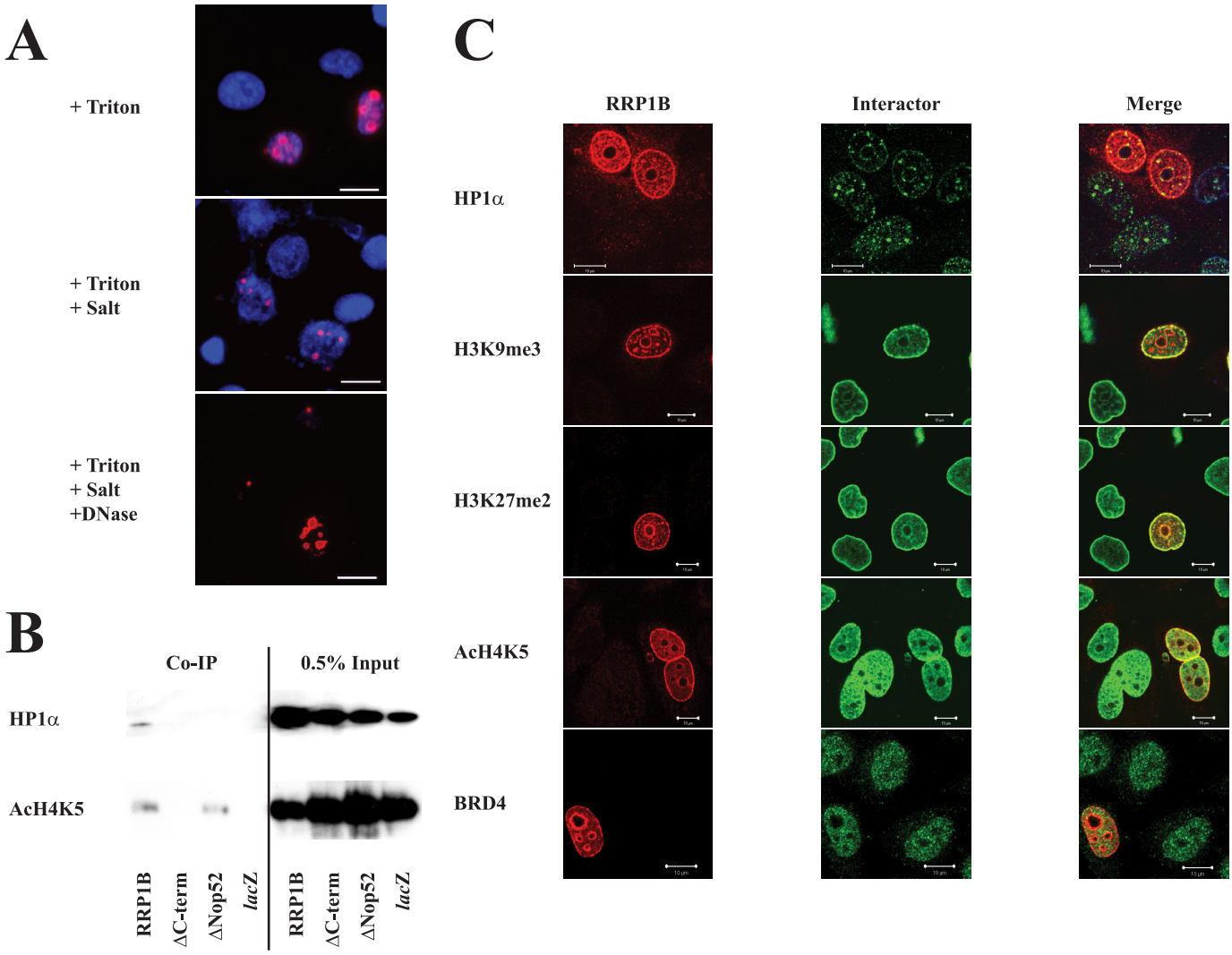

FIGURE 5. **RRP1B interacts and co-localizes with a number of heterochromatin- and euchromatin-associated proteins.** *A*, sequential nuclear extraction confirms that nucleolar RRP1B associates with DNA and the nuclear matrix. *B*, co-IP was used to define interactions with either HP1α or AcH4K5. HeLa cells (HP1α co-IP) or HEK293 (AcH4K5 co-IP) were transiently transfected with full-length RRP1B. Following immunoprecipitation performed with chromatin preparations, interactions were defined by blotting for the endogenous binding partner. HeLa cells were used for the HP1α co-IP due to the higher endogenous levels of this protein. *C*, indirect immunofluorescence was performed to confirm the interaction of RRP1B with these chromatin-associated proteins. HeLa cells were co-stained for ectopically expressed full-length RRP1B (*red*) and the endogenous interactor (*green*), and localization was confirmed using confocal microscopy. *Bar*, 10 μm.

this transcript is differentially regulated by the two allelic variants.

DISCUSSION

The data presented here confirm the role of RRP1B dysregulation in tumor progression and metastasis and also offer some insight into the mechanism of action of this metastasis-associated factor. Initially, we focused upon refining our earlier observations of the effects of ectopic expression of *Rrp1b* upon the highly metastatic Mvt-1 cell line (14). We had previously demonstrated that *Rrp1b* activation suppressed the metastatic potential of the Mvt-1 line. Furthermore, we demonstrated that not only does *Rrp1b* activation have profound effects upon global gene expression, with over 1,300 genes being dysregulated on microarray analysis, but also that these transcriptional changes can be used to develop an "*Rrp1b* activation signature." This microarray-derived activation signature was proven to predict survival in a very well characterized Dutch breast cancer microarray expression data set (14). In the current study, the *Rrp1b* activation signature accurately predicted outcome in three publicly available breast cancer expression data sets, proving the prognostic power of this expression profile. The fourth data set (23), however, was somewhat different from its counterparts in that the end point for this study was recurrence of neoplastic disease, either locally or in a distant organ. It is therefore plausible that the differences in study end points in different data sets could influence the prognostic value of the *Rrp1b* signature. Specifically, tumor recurrence does not exactly equate to likelihood of overall survival (*i.e.* the length of survival is rather variable following the detection of clinically overt recurrence).

The cellular localization of RRP1B is particularly interesting, given the profound and clinically relevant effects that *Rrp1b* dysregulation has upon global gene expression. Specifically,

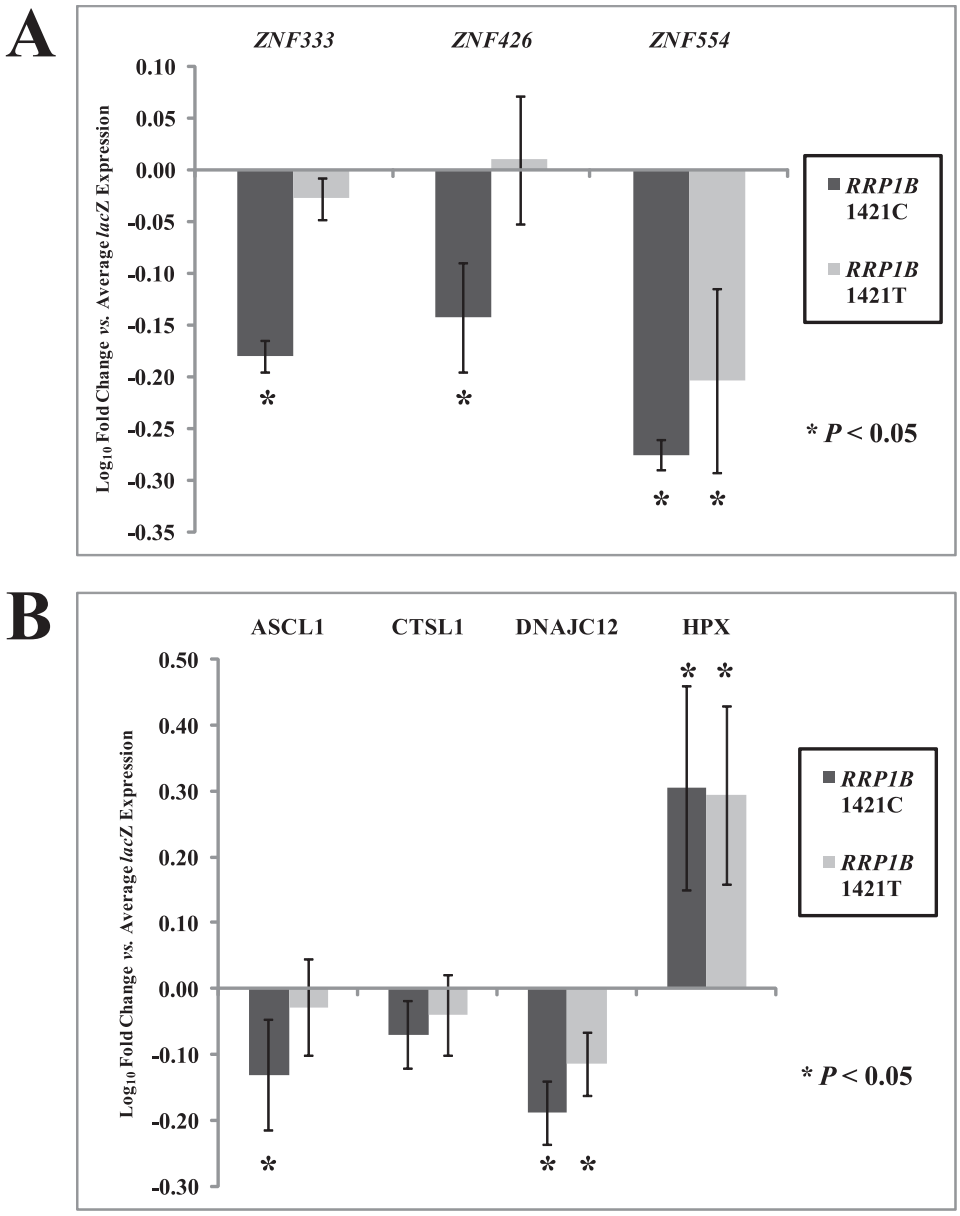

FIGURE 6. **The effect of ectopic expression of either the wild type (1421C) or variant (1421T) *RRP1B* alleles on the expression of transcripts regulated by RRP1B interactors in HeLa cells.** qPCR analysis was performed to determine the effect of *RRP1B* variant allele expression upon the transcriptional targets of TRIM28 (*A*) or CSDA (*B*). Transcript expression levels were compared between HeLa cells ectopically expressing either *RRP1B* allelic variant or *lacZ* control cultures. Significance levels were calculated by comparing relative transcript quantities of *RRP1B*-transfected and *lacZ*-transfected HeLa cells using the Mann-Whitney *U* test. Significant comparisons at the $p < 0.05$ level are marked with an *asterisk*.

localization of RRP1B to the nuclear periphery on co-IF gives some insight into how this factor may regulate transcription, since repositioning of genes to the nuclear lamina has been shown to induce transcriptional repression (32). Also, the human HP1 protein, which is a potent inducer of heterochromatinization and an RRP1B interactor, physically interacts with the receptor for the inner nuclear membrane component, LMNB1 (33). Co-IF analysis reveals that ectopic expression of full-length RRP1B induces repositioning of HP1α to the nuclear lamina compared with untransfected cells (Fig. 5*B*, *top center*; compare transfected and untransfected cells in the same *image*). This gives the impression that RRP1B may well induce chromatin reorganization, which may well be another mechanism by which RRP1B impacts global gene expression. Future experimentation will determine whether this is the case.

By defining protein-protein interactions, we have also been able to derive further insight into the function of this metastasis-related factor. We screened for RRP1B interactors using the TAP assay and found that a diverse range of proteins interact with this factor (Table 1). Interestingly, a number of these have been shown to display abnormal expression in advanced tumors (*e.g.* NPM1 (34), PARP1 (35), and NCL (36)). Furthermore, the transcriptional repressor and chromatin remodeler TRIM28 has been shown to be a novel metastasis-associated protein (37), with TRIM28 being overexpressed in both high metastatic potential metastatic cell lines and tissue sections derived from poor outcome breast carcinomas. Significantly, again in terms of the effects that RRP1B has upon global gene expression, all of these factors are nucleosome-binding proteins that have some form of chromatin remodeling capabilities. For example, both NCL and NPM1 have been shown to have histone chaperone activity (reviewed by De Koning *et al.* (38)). The interaction between RRP1B and these histone chaperones opens many potential avenues for the future investigation.

We also demonstrated that RRP1B interacts with markers of heterochromatin (*e.g.* TRIM28 and HP1α) and actively transcribed euchromatin (*e.g.* AcH4K5), implying that this factor plays a dynamic role in the modulation of gene expression. The interaction between RRP1B and H4K5ac is particularly interesting, since the previously described metastasis efficiency modifier BRD4 also binds this form of acetylated histone H4. Both RRP1B (14) and BRD4 (16) physically interact with and modulate the enzymatic activity of the metastasis efficiency modifier SIPA1. Also, *Rrp1b* and *Brd4* share a transcriptional relationship, at least in the Mvt-1 cell line, with ectopic expression of *Rrp1b* activating the expression of *Brd4* and ectopic expression of *Brd4* suppressing the expression of *Rrp1b* (15). It is interesting to note that a number of RRP1B interactors have functional effects upon BRD4-related transcriptional pathways. For example, P-TEFb-mediated RNA polymerase II transcription is stimulated by the binding of BRD4 to acetylated

histone H3 and H4 (29). The RRP1B interactor NPM1 stimulates transcription through its actions as a negative regulator of the inhibitor of P-TEFb, HEXIM1 (39). Future experiments will focus upon expanding the nature of the relationship between RRP1B and BRD4, with particular emphasis placed upon how RRP1B impacts P-TEFb-mediated RNA polymerase II transcription.

Finally, we explored the functional relevance of the *RRP1B* 1421C (Pro^{436}) wild type and 1421T (Leu^{436}) variant alleles and their differing relationships with various RRP1B interactors. We have previously demonstrated that the variant allele of this polymorphism is associated with a better outcome in multiple breast cancer cohorts (14). Here, we transiently expressed each allelic variant in HeLa cells and quantified the expression of transcripts regulated by transcription factors and RRP1B interactors, TRIM28 and CSDA. O'Geen *et al.* (30) demonstrated that TRIM28 (KAP1), a factor that is known to act as a transcriptional co-repressor with KRAB-ZNF transcription factors, facilitates an autoregulatory loop that suppresses KRAB-ZNF expression. We have subsequently demonstrated that the wild type *RRP1B* allele but not the variant allele can suppress the expression of the TRIM28-regulated KRAB-ZNF factors *ZNF333* or *ZNF426*. This occurrence may well, in part, underlie the protective effect of the variant *RRP1B* allele in breast cancer metastasis. It should be noted that members of the KRAB-ZNF family of transcriptional repressors have particularly broad effects upon gene expression, which is a consequence of the frequencies of their core DNA binding sequences (*e.g.* ZNF333 binds to the sequence ATAAT) (40). Therefore, global forms of analysis, including investigation of local chromatin structure at KRAB-ZNF-regulated promoters in response to dysregulation of *RRP1B*, will be required to fully comprehend the significance of this result.

It is obvious, however, from studying the list of RRP1B interactors on TAP analysis (Table 1) that RRP1B probably has functions beyond the regulation of transcription and chromatin structure. It certainly appears apparent that RRP1B is involved in the process of ribosome biogenesis, since it interacts with a number of components of the large ribosomal subunit (*e.g.* RPL4, RPL5, RPL10A, and RPLP0). Additionally, it is probable that RRP1B is involved in the rRNA generation and processing, since various RRP1B interactors (*e.g.* NPM1 (41) and NCL (42)) regulate pre-rRNA processing. Additionally, RRP1B interacts with a number of proteins involved in alternative mRNA splicing, including SFRS1 (SF2/ASF) and hnRNPA1, both of which have been shown to interact and regulate alternative splicing in a tissue-specific manner (43). Given that dysregulation of both ribosome biogenesis (reviewed in Ref. 44) and alternative mRNA splicing (reviewed in Ref. 45) are features of advanced neoplasia, it will be particularly interesting to determine the extent to which RRP1B impacts these processes.

In conclusion, we have confirmed that a microarray gene expression signature induced by ectopically expressing *Rrp1b* in the highly metastatic Mvt-1 cell line can be used to accurately predict survival in multiple breast cancer data sets. Functional analysis has given us some insight into how RRP1B dysregulation impacts the expression of metastasis-related transcripts. Specifically, we demonstrate that RRP1B physically interacts with a variety of nucleosome binding proteins, all of which have been demonstrated to be regulators of chromatin structure and transcription. In fact, it appears that RRP1B itself is a chromatin-associated protein by virtue of its interactions with histone variants and various heterochromatin-associated proteins. It is interesting that RRP1B seems to interact with both heterochromatin and euchromatin-associated factors. The significance of this is uncertain at present, although it does suggest that RRP1B probably plays a dynamic role in the regulation of gene expression.

Acknowledgments—We thank Dr. Tom Misteli (NCI, National Institutes of Health, Bethesda, MD) for advice regarding experimentation and critical review of the manuscript, Dr. Tae-Aug Kim (NCI, National Institutes of Health) for assistance with the nuclear matrix extraction experiment, and Dr. Spyros Georgatos (University of Ioannina, Greece) for help with performing the RRP1B-HP1α co-IP.

REFERENCES

1. Rae, J. M., Skaar, T. C., Hilsenbeck, S. G., and Oesterreich, S. (2008) *Breast Cancer Res.* **10,** 301
2. Jemal, A., Tiwari, R. C., Murray, T., Ghafoor, A., Samuels, A., Ward, E., Feuer, E. J., and Thun, M. J. (2004) *CA Cancer J. Clin.* **54,** 8–29
3. Guy, C. T., Cardiff, R. D., and Muller, W. J. (1992) *Mol. Cell. Biol.* **12,** 954–961
4. Lifsted, T., Le Voyer, T., Williams, M., Muller, W., Klein-Szanto, A., Buetow, K. H., and Hunter, K. W. (1998) *Int. J. Cancer* **77,** 640–644
5. Park, Y. G., Zhao, X., Lesueur, F., Lowy, D. R., Lancaster, M., Pharoah, P., Qian, X., and Hunter, K. W. (2005) *Nat. Genet.* **37,** 1055–1062
6. Crawford, N. P., Ziogas, A., Peel, D. J., Hess, J., Anton-Culver, H., and Hunter, K. W. (2006) *Breast Cancer Res.* **8,** R16
7. van de Vijver, M. J., He, Y. D., van't Veer, L. J., Dai, H., Hart, A. A., Voskuil, D. W., Schreiber, G. J., Peterse, J. L., Roberts, C., Marton, M. J., Parrish, M., Atsma, D., Witteveen, A., Glas, A., Delahaye, L., van der Velde, T., Bartelink, H., Rodenhuis, S., Rutgers, E. T., Friend, S. H., and Bernards, R. (2002) *N. Engl. J. Med.* **347,** 1999–2009
8. van't Veer, L. J., Dai, H., van de Vijver, M. J., He, Y. D., Hart, A. A., Mao, M., Peterse, H. L., van der Kooy, K., Marton, M. J., Witteveen, A. T., Schreiber, G. J., Kerkhoven, R. M., Roberts, C., Linsley, P. S., Bernards, R., and Friend, S. H. (2002) *Nature* **415,** 530–536
9. Ramaswamy, S., Ross, K. N., Lander, E. S., and Golub, T. R. (2003) *Nat. Genet.* **33,** 49–54
10. Yang, H., Rouse, J., Lukes, L., Lancaster, M., Veenstra, T., Zhou, M., Shi, Y., Park, Y. G., and Hunter, K. (2004) *Clin. Exp. Metastasis* **21,** 719–735
11. Yang, H., Crawford, N., Lukes, L., Finney, R., Lancaster, M., and Hunter, K. W. (2005) *Clin. Exp. Metastasis* **22,** 593–603
12. Lukes, L., Crawford, N. P., Walker, R., and Hunter, K. W. (2009) *Cancer Res.* **69,** 310–318
13. Mucenski, M. L., Taylor, B. A., Jenkins, N. A., and Copeland, N. G. (1986) *Mol. Cell. Biol.* **6,** 4236–4243
14. Crawford, N. P., Qian, X., Ziogas, A., Papageorge, A. G., Boersma, B. J., Walker, R. C., Lukes, L., Rowe, W. L., Zhang, J., Ambs, S., Lowy, D. R., Anton-Culver, H., and Hunter, K. W. (2007) *PLoS Genet.* **3,** e214
15. Crawford, N. P., Walker, R. C., Lukes, L., Officewala, J. S., Williams, R. W., and Hunter, K. W. (2008) *Clin. Exp. Metastasis* **25,** 357–369
16. Farina, A., Hattori, M., Qin, J., Nakatani, Y., Minato, N., and Ozato, K. (2004) *Mol. Cell. Biol.* **24,** 9059–9069
17. Crawford, N. P., Alsarraj, J., Lukes, L., Walker, R. C., Officewala, J. S., Yang, H. H., Lee, M. P., Ozato, K., and Hunter, K. W. (2008) *Proc. Natl. Acad. Sci. U.S.A.* **105,** 6380–6385
18. Gingras, A. C., Caballero, M., Zarske, M., Sanchez, A., Hazbun, T. R., Fields, S., Sonenberg, N., Hafen, E., Raught, B., and Aebersold, R. (2005) *Mol. Cell Proteomics* **4,** 1725–1740
19. Vecerová, J., Koberna, K., Malínsky, J., Soutoglou, E., Sullivan, T., Stewart,

C. L., Raska, I., and Misteli, T. (2004) *Mol. Biol. Cell* **15,** 4904–4910
20. Pawitan, Y., Björhle, J., Amler, L., Borg, A. L., Egyhazi, S., Hall, P., Han, X., Holmberg, L., Huang, F., Klaar, S., Liu, E. T., Miller, L., Nordgren, H., Ploner, A., Sandelin, K., Shaw, P. M., Smeds, J., Skoog, L., Wedrén, S., and Bergh, J. (2005) *Breast Cancer Res.* **7,** R953–R964
21. Miller, L. D., Smeds, J., George, J., Vega, V. B., Vergara, L., Ploner, A., Pawitan, Y., Hall, P., Klaar, S., Liu, E. T., and Bergh, J. (2005) *Proc. Natl. Acad. Sci. U.S.A.* **102,** 13550–13555
22. Ivshina, A. V., George, J., Senko, O., Mow, B., Putti, T. C., Smeds, J., Lindahl, T., Pawitan, Y., Hall, P., Nordgren, H., Wong, J. E., Liu, E. T., Bergh, J., Kuznetsov, V. A., and Miller, L. D. (2006) *Cancer Res.* **66,** 10292–10301
23. Wang, Y., Klijn, J. G., Zhang, Y., Sieuwerts, A. M., Look, M. P., Yang, F., Talantov, D., Timmermans, M., Meijer-van Gelder, M. E., Yu, J., Jatkoe, T., Berns, E. M., Atkins, D., and Foekens, J. A. (2005) *Lancet* **365,** 671–679
24. Zhou, M., and Cui, Y. (2004) *In Silico Biol.* **4,** 323–333
25. Andersen, J. S., Lyon, C. E., Fox, A. H., Leung, A. K., Lam, Y. W., Steen, H., Mann, M., and Lamond, A. I. (2002) *Curr. Biol.* **12,** 1–11
26. Horsey, E. W., Jakovljevic, J., Miles, T. D., Harnpicharnchai, P., and Woolford, J. L., Jr. (2004) *RNA* **10,** 813–827
27. Cokol, M., Nair, R., and Rost, B. (2000) *EMBO Rep.* **1,** 411–415
28. Dey, A., Chitsaz, F., Abbasi, A., Misteli, T., and Ozato, K. (2003) *Proc. Natl. Acad. Sci. U.S.A.* **100,** 8758–8763
29. Jang, M. K., Mochizuki, K., Zhou, M., Jeong, H. S., Brady, J. N., and Ozato, K. (2005) *Mol. Cell* **19,** 523–534
30. O'Geen, H., Squazzo, S. L., Iyengar, S., Blahnik, K., Rinn, J. L., Chang, H. Y., Green, R., and Farnham, P. J. (2007) *PLoS Genet.* **3,** e89
31. Tobita, H., Kajino, K., Inami, K., Kano, S., Yasen, M., Imamura, O., Kinoshita, Y., and Hino, O. (2006) *Int. J. Oncol.* **29,** 673–679
32. Reddy, K. L., Zullo, J. M., Bertolino, E., and Singh, H. (2008) *Nature* **452,** 243–247
33. Ye, Q., and Worman, H. J. (1996) *J. Biol. Chem.* **271,** 14653–14656
34. Grisendi, S., Mecucci, C., Falini, B., and Pandolfi, P. P. (2006) *Nat. Rev. Cancer* **6,** 493–505
35. Peralta-Leal, A., Rodríguez, M. I., and Oliver, F. J. (2008) *Clin. Transl. Oncol.* **10,** 318–323
36. Storck, S., Shukla, M., Dimitrov, S., and Bouvet, P. (2007) *Subcell. Biochem.* **41,** 125–144
37. Ho, J., Kong, J. W., Choong, L. Y., Loh, M. C., Toy, W., Chong, P. K., Wong, C. H., Wong, C. Y., Shah, N., and Lim, Y. P. (2009) *J. Proteome Res.* **8,** 583–594
38. De Koning, L., Corpet, A., Haber, J. E., and Almouzni, G. (2007) *Nat. Struct. Mol. Biol.* **14,** 997–1007
39. Gurumurthy, M., Tan, C. H., Ng, R., Zeiger, L., Lau, J., Lee, J., Dey, A., Philp, R., Li, Q., Lim, T. M., Price, D. H., Lane, D. P., and Chao, S. H. (2008) *J. Mol. Biol.* **378,** 302–317
40. Jing, Z., Liu, Y., Dong, M., Hu, S., and Huang, S. (2004) *J. Biochem. Mol. Biol.* **37,** 663–670
41. Dumbar, T. S., Gentry, G. A., and Olson, M. O. (1989) *Biochemistry* **28,** 9495–9501
42. Tuteja, R., and Tuteja, N. (1998) *Crit. Rev. Biochem. Mol. Biol.* **33,** 407–436
43. Pollard, A. J., Krainer, A. R., Robson, S. C., and Europe-Finner, G. N. (2002) *J. Biol. Chem.* **277,** 15241–15251
44. Montanaro, L., Treré, D., and Derenzini, M. (2008) *Am. J. Pathol.* **173,** 301–310
45. Skotheim, R. I., and Nees, M. (2007) *Int. J. Biochem. Cell Biol.* **39,** 1432–1449